Proceedings of DETC 2003
2003 ASME Design Engineering Technical Conferences
September 2-6, 2003, Chicago, Illinois, USA

DETC2003-48516

HOPF BIFURCATION IN A DISK-SHAPED NEMS

Maxim Zalalutdinov, Jeevak Parpia
Physics Department
Cornell University
Ithaca NY 14853

Keith Aubin, Harold Craighead,
School of Applied and
Engineering Physics
Cornell University
Ithaca NY 14853

Tuncay Alan, Alan Zehnder, Richard Rand
Department of Theoretical
and Applied Mechanics
Cornell University
Ithaca NY 14853

ABSTRACT

Self-sustained mechanical vibrations of a disc-type microfabricated resonator were experimentally observed when a continuous wave (CW) laser beam was focused on the periphery of the disc (for a 40 μm diameter resonator, natural frequency 0.89MHz, the laser power above a 250 W threshold was required). A theoretical model for self-oscillatory behavior has been developed based on FEM analysis of a stress pattern created within the resonator by the focused laser beam. This model accounts for the fact that the amount of absorbed laser light is modulated due to the motion of the resonator through the optical interferometric pattern. Analytical study reveals the presence of a Hopf-type bifurcation with a critical laser power close to the experimentally observed value. Harmonic balance analysis indicates the existence of a stable limit cycle in the phase plane determining the amplitude of self-oscillations.

INTRODUCTION

Micro- and nano-mechanical (NEMS) resonators have many potential applications in systems such as pressure and temperature sensors, [1,2], accelerometers [1,3], scanning force microscopes [4,5], and mass detectors [6]. In a typical application the frequency carries the information on the quantity of interest (mass, temperature, pressure, etc...). Nano-mechanical resonators also have potential applications in radio frequency communications systems, providing nanoscale solutions for functions such as filtering and signal conversion [7,8].

Some of the challenges to using NEMS resonators include drive, signal transduction and attainment of high quality factor. It is known that parametric pumping, i.e. modulation of resonator stiffness, can be used to drive NEMS resonators and to increase their effective quality factor and hence system sensitivity [9]. Electrostatic [9-11], magnetic [12], and mechanical [13] pumping for parametric amplification in MEMS are common approaches. The mechanics of parametric drive of electrostatic torsional oscillators has been studied extensively [14].

It has been recently discovered that optical excitation can be used to drive and to parametrically amplify vibrations of NEMS oscillators, [15-18]. This discovery opens up many new potential applications of NEMS resonators. However, to exploit these opportunities the mechanics of optically driven NEMS devices must be well understood. Combining thermo-mechanical finite element analysis with numerical solutions of a dynamical model of the oscillator, prior studies identified the mechanisms for parametric excitation and self-oscillation [15-17]. Here we introduce an additional feature in the model to account for static deflection of the disks due to heating. This addition brings the predictions of the model into much better agreement with the experiments. We will also concentrate on using analytical approaches to explore simplified models of optically driven NEMS resonators.

The geometry and fabrication of the devices will be described, followed by an overview of the experimental methods and observations. Finite element analyses used to determine system parameters will be described. Then a model of the system will be developed and explored and to the extent possible, its predictions compared to experimental results.

OSCILLATOR GEOMETRY, FABRICATION AND EXPERIMENTAL OBSERVATIONS

Commercially available silicon-on-insulator (SOI) wafers with a 250 nm thick silicon layer on top of a 1 μm silicon oxide layer were used for the microfabrication. Discs of radii, R, from 5 to 20 μm were defined by electron-beam lithography followed by a dry etch through the top silicon layer. Dipping the resulting structure into hydrofluoric acid undercuts the silicon oxide starting from the disc's periphery toward the center. By timing this wet etch, the diameter of the remaining column of the silicon oxide, which supports the released silicon disc, can be varied. In this paper we present data obtained with $R = 20\mu m$ discs supported by the SiO_2 pillars with diameter $6.7\mu m$, see Fig.1. After a critical point drying (CPD) process, samples were bonded to a piezoceramic transducer and placed into a high vacuum chamber ($P = 10^-7$ Torr) for testing. All measurements were done at room temperature.

Motion of the disk is detected using the interferometric setup [19] shown in Fig.2, that uses a He-Ne laser beam focused on the surface of the disc. The disk is thin enough that light can pass through the disk, reflect from the substrate and then interfere with light reflected from the disk, forming a Fabry-Perot type interferometer. The net reflected signal, measured using an AC coupled photodetector, is a periodic function of the disk deflection. The net light absorbed by the disk is also a periodic function of the deflection. Thus, as the disk moves, it passes continuously into and out of regions of higher and lower light absorption. Incident light intensity can be controlled with an electro-optic modulator. An AC voltage applied to the piezoceramic transducer to which the wafer is bonded, can be used to excite the NEMS oscillators.

Focusing a low power continuous wave (CW) HeNe laser onto a 5 μm spot on the periphery of the disk, and exciting the oscillator with the piezo-ceramic transducer, the resonant frequency of the disk was measured as a function of laser light intensity for several modes of vibration. As seen in Fig.3, the frequencies of the two lowest modes increase with laser power, while the frequency of the third mode decreases.

With the piezo drive switched off, when the CW laser intensity in increased beyond approximately $250\mu W$ the disk begins to self-oscillate. This is seen in Fig.4 where the amplitude of motion increases abruptly once the threshold laser power is exceeded. Additional experimental observations are discussed in refs. [15-18].

FINITE ELEMENT MODELING AND MECHANISMS FOR SELF-EXCITATION

Two mechanisms, both involving light absorption, heating and thermal stress are causing the self-excitation. Depending on the oscillator's deflection, from 5 to 25% of the incident laser light is absorbed, increasing the temperature of the disk. The disk, unable to thermally expand at its center due to the SiO_2 pillar goes into tension in the radial direction and compression in the hoop direction. The radial tension stiffens the disk for vibration modes involving primarily radial bending (modes 1 and 2) and softens the disk for modes involving primarily hoop bending (mode 3). This is verified by the finite element results of Fig.5 that show the temperature and thermal stress field for steady state heating. Modal analyses were performed before and after heating. The modal shapes are shown in Fig.1d. Note that since Si is a cubic material there are two modes with slightly different frequencies, rotated by 45^o with respect to each other, that are identical in shape to the last mode shown in Fig.1d. The change in resonant frequency versus incident laser power (assuming 25 % absorption) is plotted in Fig.3 for the first three modes.

As the disk oscillates, it is subject to modulated laser heating, due either to passing through the absorption interference fringes or due to external modulation of the laser. In either case, since the disk is so small it can heat and cool in response to the modulated heating. Note that the disk's thermal time constant is about $2\mu s$ and its period of vibration about 1 μs. Thus, as the disk oscillates its temperature is modulated, resulting in modulation of the stiffness. If at the equilibrium position the disk lies at either a maximum or minimum of the absorption fringes, then due to passing through the absorption interference fringes the modulation of stiffness is always at a 2:1 ratio to the motion, resulting in Mathieu-equation-like parametric pumping of the system. Note that the larger the amplitude of motion, the larger the modulation of stiffness, unlike the canonical Mathieu system in which the change in spring stiffness is independent of amplitude of motion.

In addition to modulation of the disk's stiffness during motion, laser heating can cause a direct deflection of the disk. Larger diameter disks, made using the same process clearly show that the disks are curved due to the release of residual stresses in the Si layer during fabrication. Furthermore, the deflection is large enough that it can be measured using interference microscopy. Using the deflection from a disk of diameter $89\mu m$, the residual stresses in the Si were estimated, and then applied in an FEM model to the $40\mu m$ disk to estimate its initial shape. Through this procedure we estimate that the $40\mu m$ disk is curved by about $100nm$.

A 3D FEM model of the curved disk was built and subjected to steady state and modulated heating over a $5\mu m$

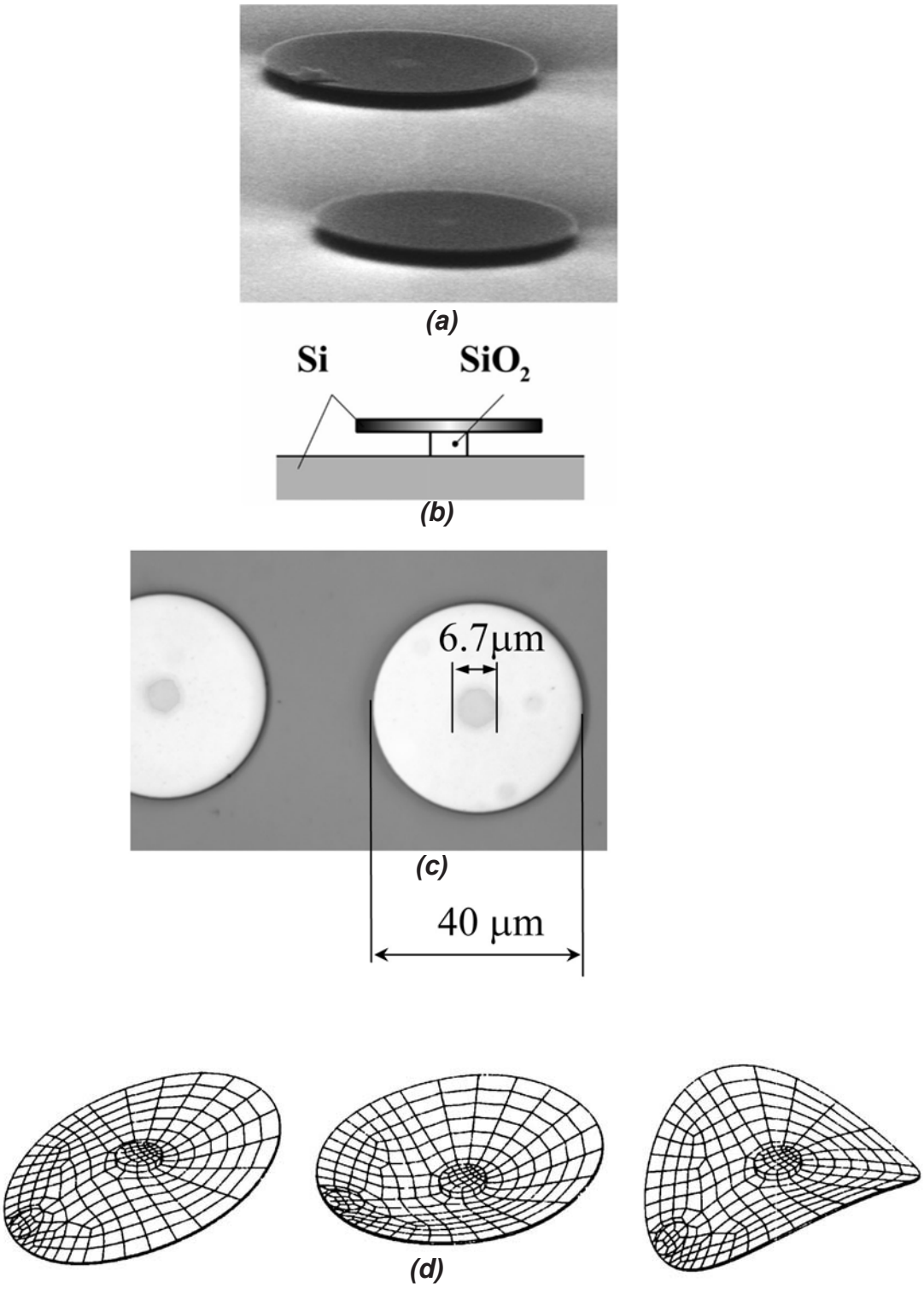

Figure 1: (a) SEM images of disk-shaped oscillator, (b) schematic, (c) optical images, (d) first three modes of vibration

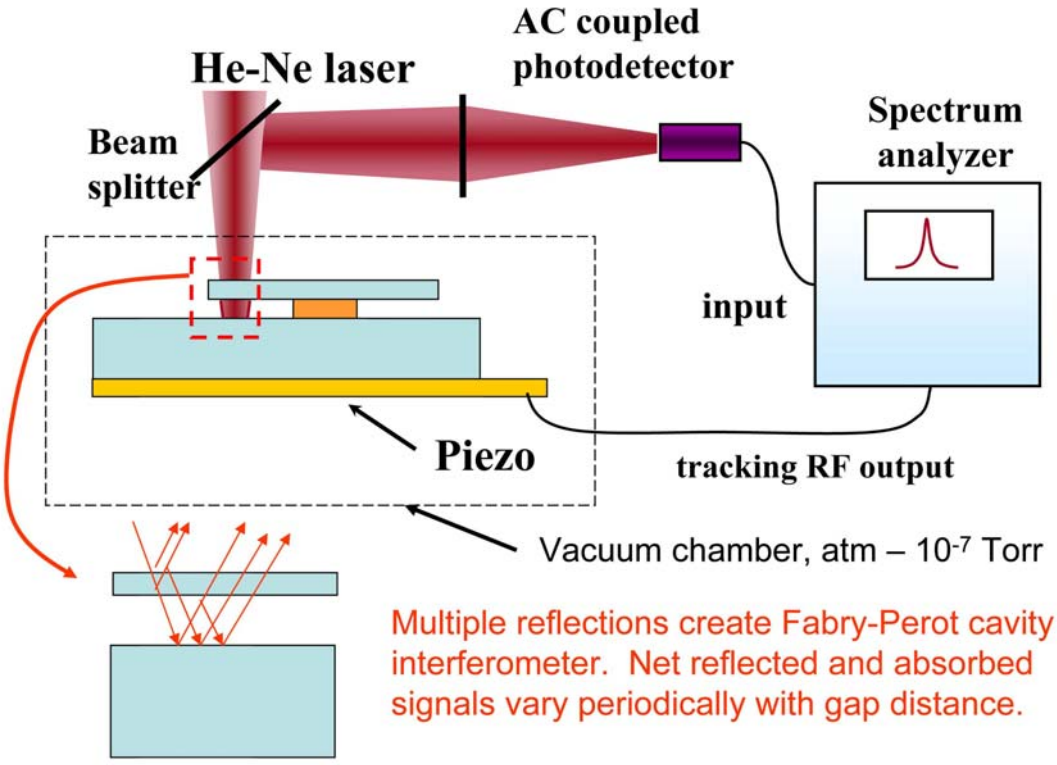

Figure 2: Experimental setup.

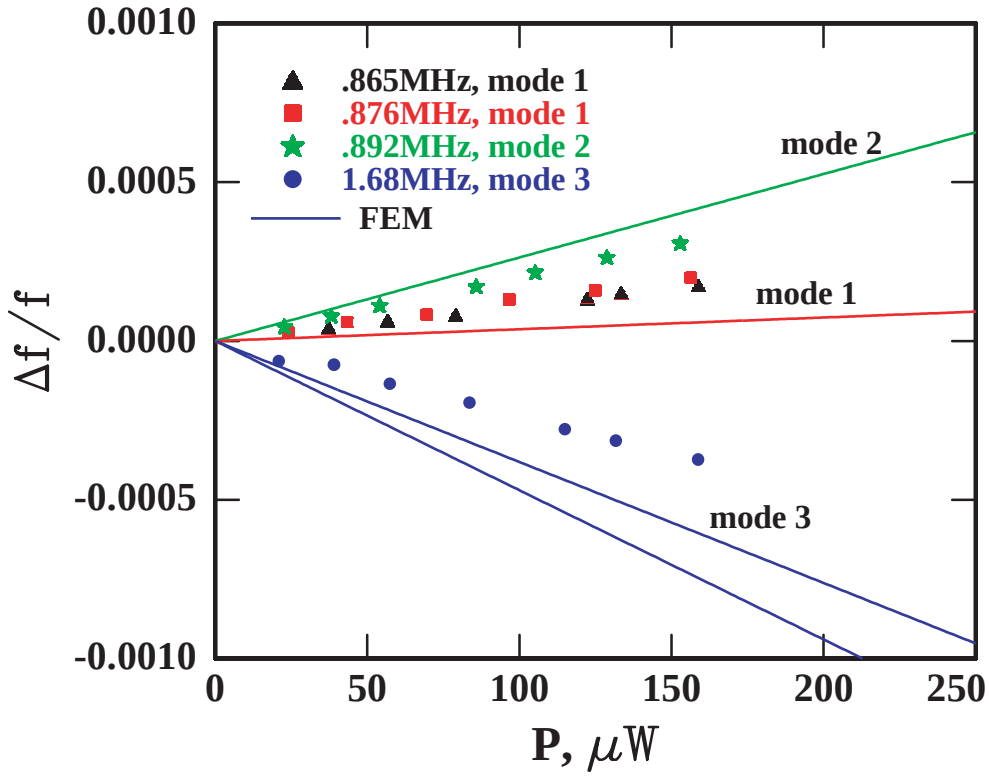

Figure 3: Relative shift in frequencies versus incident laser power, below threshold for self-oscillation. Points are experimental measurements from several repeats. Solid lines from FEM simulation. Mode numbers refer to mode shapes in Figure 1. Note that mode shape 3 in Figure 1 actually has two modes rotated 45^o to each other, thus there are two FEM lines for this mode.

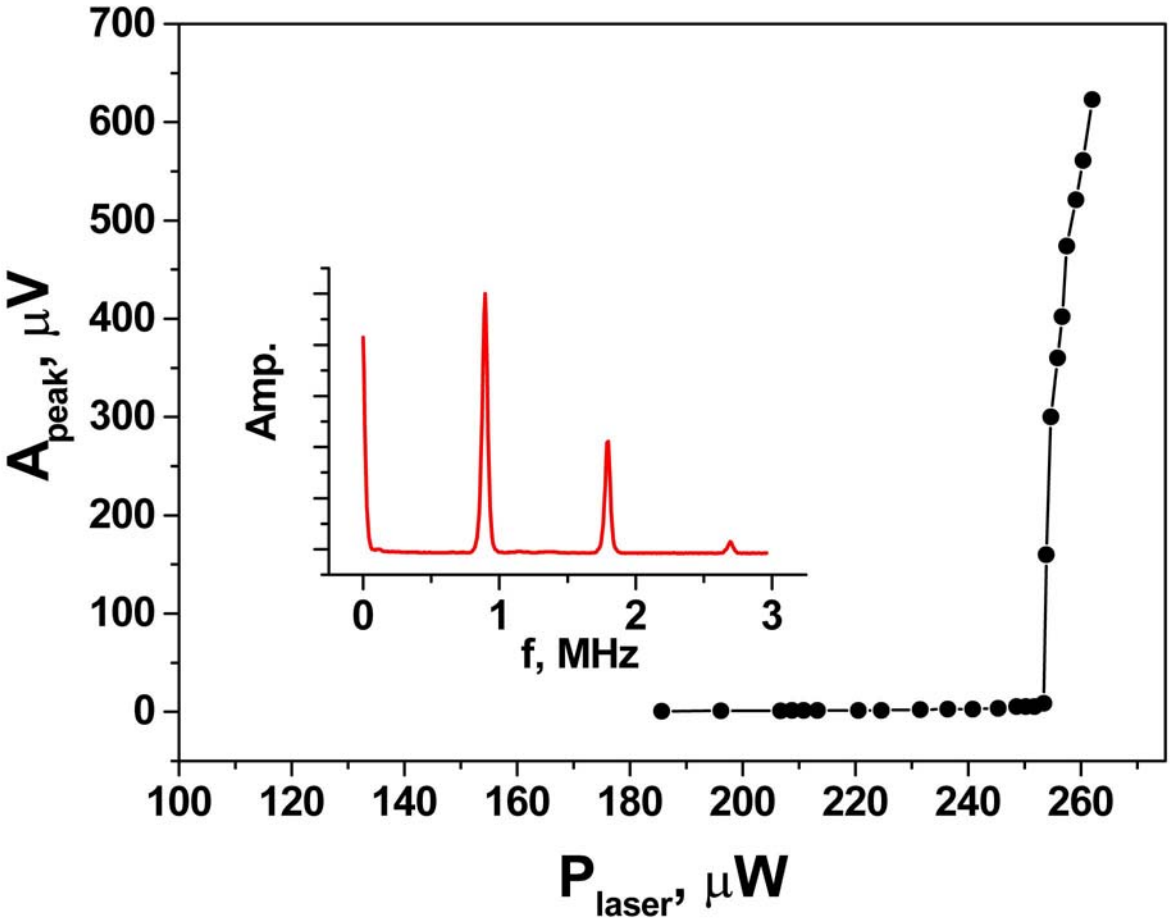

Figure 4: Amplitude of signal to photodector versus incident laser power. Inset shows spectrum at a power above $250\mu W$. The multiple peaks are due to nonlinearity in the relationship between reflected signal and deflection.

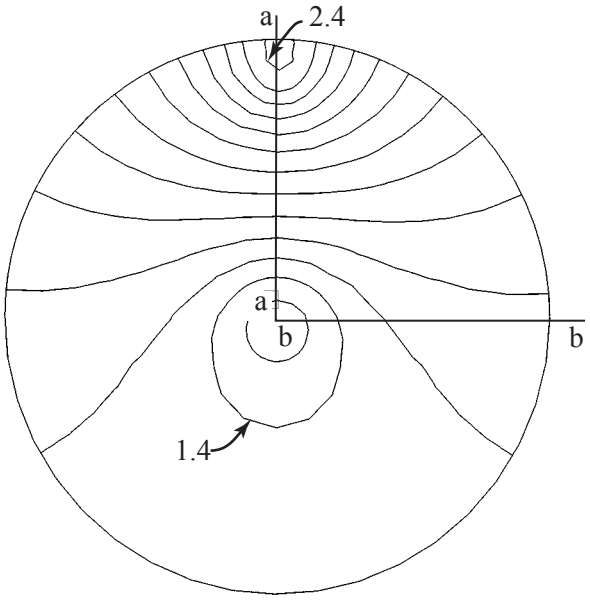

(a)

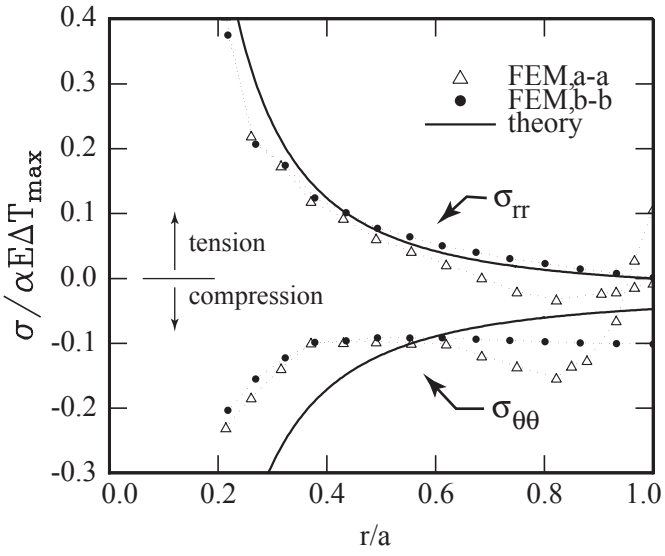

(b)

Figure 5: FEM results for steady heating, assuming a $260\mu W$ laser spot, focused on a $5\mu m$ diameter region on the periphery of the disk, and assuming 25 absorption of light. Mechanical and thermal properties for FEM simulation are given in Table 1. (a) Increase in temperature, ^{o}C. (b) Radial and hoop stresses along sections a-a and b-b. Solid line shows stress field for a disk heated uniformly to δT_{max}

.

	Si (100)Properties [20, 21]
E	130 GPa
ν	.279
μ	79.1 GPa
ρ	2420 kg/m^3
k	170 W/m K
c	712 J/kg K
α	2.5 $\times 10^{-5}$/K
dE/dT	-130 $\times 10^{-4}$ GPa/K
dμ/dT	-79.1 $\times 10^{-4}$ GPa/K

Table 1. Properties of Si(100)

spot. From these calculations, the deflection of the disk due to modulated heating and thermal expansion could be determined. Note that if the disk was flat it would deflect much less. In this case the deflection would be due only to the gradient of temperature through the thickness. This gradient, however is very small due to the very fast time constant for conduction through the thickness ($6 \times 10^{-4} \mu s$) relative to the $1\mu s$ period. In larger MEMS systems bending of beams due to through the thickness thermal expansion gradient has been identified as leading to self-oscillation and bi-stability of equilibrium deflections [22,23]. Note also that in the current problem, the deflection due to photon pressure is negligible relative to the motion caused by thermal expansion of the curved disk.

MATHEMATICAL MODEL

We model the system as a lumped thermal mass and single degree of freedom oscillator. In the thermal problem the disk heats up due to absorbed laser light and cools according to Newton's law of cooling, i.e. the rate of heat loss is proportional to the temperature above ambient. The absorbed laser light can be modulated externally by modulating the incident laser and internally by the disk moving through the interference fringes. In the mechanical problem the bending up or down of the curved disk due to laser heating is treated as a base excitation. Modulation of the stiffness due to dynamic temperature changes is assumed to be proportional to the temperature change. Making these assumptions, and assuming that there is no other external drive in the system, the motion and heating of the disk oscillator can be modeled using the following coupled set of differential equations,

$$\ddot{z} + \frac{1}{Q}(\dot{z} - D\dot{T}) + (1 + cT)(z - DT + \beta(z - DT)^3) = 0 \quad (1)$$

$$\dot{T} + BT = AP(1 + \phi \sin \Omega t)(\alpha + \gamma \sin^2 2\pi(z - z_0)) \quad (2)$$

where z is the deflection normalized by wavelength of laser light, Q is the quality factor, c is the relative change in spring constant per unit temperature change, T is temperature change in ^oC, β is the nonlinearity in the disk's stiffness, D is the deflection of the disk due to heating, per unit temperature change, B represents the disk's overall thermal conductivity, A its overall thermal mass, P the incident laser power in μW, ϕ the fraction of modulation of the incident laser beam, Ω the frequency of modulation of the incident laser beam, α is the minimum value of absorption, γ is the contrast in the absorption curve, and z_0 represents the disk's equilibrium position relative to the absorption interference curve. Note that the $\sin^2 2\pi(z - z_0)$ term is an approximation to the actual absorption curve. Time has been non-dimensionalized in the above system so that the frequency of small oscillations is 1. In the above system, the bending of the beam due to heating is treated as a base excitation.

Values for A and B were calculated based on the maximum temperatures calculated in FEM simulations of both steady state and modulated laser heating. Heating was modulated at frequency 2. The quality factor was estimated from experiments where the disk was piezo driven at small amplitudes. The stiffness change per temperature, c was estimated from the FEM simulation by calculating the resonant frequency change. The deflection per temperature, D was estimated from the FEM simulation by calculating the amplitude of motion due to frequency 2 modulated laser heating. The cubic non-linearity in stiffness was estimated based on experimentally observed frequency-amplitude curves. The absorption parameters, α, γ and z_0 are calculated based on the dielectric properties of the Si, its thickness and the gap thickness [20]. Note that the gap thickness depends on the initial curvature of the disk. Analyses of several sized disks have been performed. For the $40\mu m$ diameter disk the following values are *estimated*: $A = .018^oC/\mu W$, $B = .49/^oC$, $c = 3.5 \times 10^{-4}/^oC$, $D = 1.3 \times 10^{-5}/^oC$, $\beta = .38$, $Q = 10^4$, $z_0 = .06$, $\alpha = .06$, and $\gamma = .26$. These parameter values will be used in the rest of this paper. Note that D and z_0 could be positive or negative depending on whether the disk curves up or down from the substrate. The laser power P is in the

range of $0 - 1000\mu W$. The modulation depth, ϕ is from 0 to 1.

We begin by seeking an expression for the equilibrium of eqs.(1),(2) in the case of no forcing, $\phi = 0$. We also take $\alpha = 0$ in what follows. From eq.(1) this will occur when $z = DT$. Substitution into eq.(2) gives

$$z = \frac{ADP\gamma}{B} \sin^2 2\pi(z - z_0) \tag{3}$$

For typical parameter values, the quantity $\frac{ADP\gamma}{B} << 1$, yielding the following approximate expression for the equilibrium of eqs.(1),(2):

$$z_{eq} = \frac{ADP\gamma}{B} \sin^2 2\pi z_0, \qquad T_{eq} = \frac{1}{D} z_{eq} \tag{4}$$

In order to investigate the stability of the equilibrium (4), we set $z = z_{eq}+u$, $T = T_{eq}+v$ in eqs.(1),(2) and linearize in u and v. The characteristic equation of the resulting linear system may be written in the form $\lambda^3+k_2\lambda^2+k_1\lambda+k_0 = 0$. For a Hopf bifurcation, $\lambda = \pm i\omega$, which gives the condition $k_1k_2 = k_0$, yielding the following expression for P_{Hopf}:

$$\begin{aligned} P_{Hopf} &= \frac{Q + B^2Q + B}{2\pi AD\gamma(Q^2 - BQ - 1)\sin 4\pi z_0} \\ &\approx \frac{1 + B^2}{2\pi AD\gamma Q \sin 4\pi z_0} \end{aligned} \tag{5}$$

where the approximation in eq.(5) is based on the small damping assumption $Q >> 1$. When the foregoing numerical values of the parameters are substituted into eq.(5), we obtain $P_{Hopf} = 474\mu W$.
Note that the theoretical value is somewhat higher than the measured threshold for self-oscillation shown in Fig.4. This suggests that we are not estimating all the parameters in the model accurately, which is not surprising given the large number of parameters and the uncertainty in the initial curvature of the disk, which affects D and z_0 in equation 5. Nonetheless the theoretical model shows excellent qualitative agreement and predicts the threshold for self-oscillation within a factor of two.

SIMPLIFIED MODEL

In this section we investigate the dynamics of a simplified version of eqs.(1),(2). We assume $D = 0$, $\phi = 0$, $z_0 = 0$ and $\alpha = 0$, whereupon eqs.(1),(2) become:

$$\ddot{z} + \frac{1}{Q}\dot{z} + (1 + cT)(z + \beta z^3) = 0 \tag{6}$$

$$\dot{T} + BT = AP\gamma \sin^2 2\pi z \tag{7}$$

We further simplify eqs.(6),(7) by Taylor-expanding $\sin^2 2\pi z$ and keeping only the first two terms in the series:

$$\sin^2 2\pi z = 4\pi^2 z^2 - \frac{16}{3}\pi^4 z^4 + \cdots \tag{8}$$

Eqs.(6)-(8) have the equilibrium solution $z = 0$, $T = 0$. Linearizing about this solution, we see that it is a stable equilibrium.

We look for periodic solutions of eqs.(6)-(8) by using the method of harmonic balance. We set

$$z = R\cos\omega t \tag{9}$$

and substitute eq.(9) into eqs.(7),(8), which gives the following periodic expression for T:

$$T = p_1+p_2\sin 2\omega t+p_3\cos 2\omega t+p_4\sin 4\omega t+p_5\cos 4\omega t \tag{10}$$

where the constants p_i are known functions of the parameters $R, \omega, A, P, \gamma, c, \beta, Q$ and B. We substitute eqs.(9),(10) into eq.(6) and collect terms after trigonometric reduction. The method of harmonic balance requires that we set the coefficients of $\cos\omega t$ and $\sin\omega t$ to zero. This gives the relations $\omega \approx 1$ and the following equation on the amplitude R:

$$(8\pi^2 - 3\beta)R^4 - 6R^2 + \frac{3(B^2 + 4)}{\pi^2 AP\gamma Qc} = 0 \tag{11}$$

Eq.(11) is a quadratic on R^2. Assuming $8\pi^2 - 3\beta > 0$, eq.(11) will have two real positive roots for R^2 if the diskriminant is positive. This gives the following condition for eqs.(6)-(8) to have two periodic solutions:

$$\frac{AP\gamma Qc}{B^2 + 4} > \frac{8}{3} - \frac{\beta}{\pi^2} \tag{12}$$

The associated periodic motions are limit cycles. Since the equlibrium at the origin $z = 0$, $T = 0$ is stable, we are not surprised to find that the smaller limit cycle is unstable and the larger one is stable. At the critical value of parameters given by replacing the inequality in (12) by an equal sign, the two limit cycles disappear in a fold. See Fig.6.

The smaller limit cycle is born in a subcritical Hopf bifurcation as the damping $1/Q$ passes through zero.

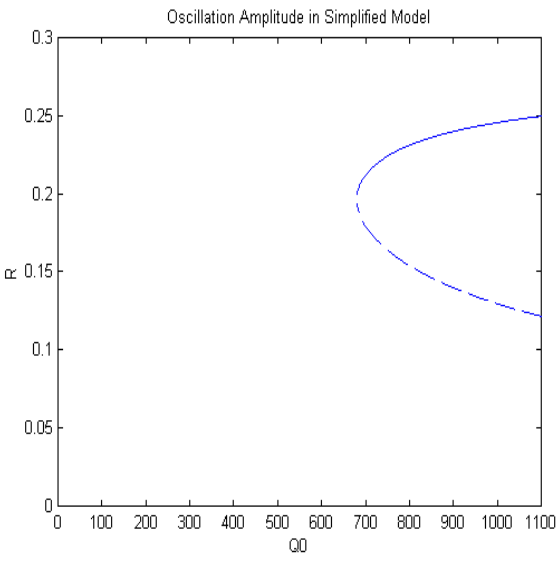

Figure 6. Oscillation amplitude R as a function of laser power P in simplified model. The larger limit cycle is stable (solid line) and the smaller limit cycle is unstable (dashed line). The equilibrium $R = 0$ is stable.

When the simplified system (6)-(8) has no damping in the z-equation, $Q \to \infty$, the origin is unstable and a stable limit cycle exists with amplitude R, where eq.(11) gives:

$$R^2 = \frac{6}{8\pi^2 - 3\beta} \tag{13}$$

Note that in this case we see from eq.(6) that no such limit cycle exists when the parameter $c = 0$. This follows because the resulting equation, $\ddot{z} + z + \beta z^3 = 0$ is conservative and the z-$\dot{z}$ phase plane is filled with concentric closed curves for $\beta > 0$. Thus we may view the limit cycle (13) as being born when the parameter c is increased from zero. This type of bifurcation is not to be confused with a Hopf, since the limit cycle first occurs with a finite amplitude, that is, it does not grow out of an equilibrium point. This situation is reminiscent of van der Pol's equation, $\ddot{z} + z - \epsilon(1 - z^2)\dot{z} = 0$, which exhibits a limit cycle of radius 2 for small values of ϵ.

CONCLUSIONS

A theoretical model for the experimentally observed self-oscillations of disk-type NEMS resonators due to CW laser irradiation was constructed. FEM simulations were employed to determine the model parameters describing thermomechanical effects in the resonator due to the laser beam. Both parametric (variation of the effective spring constant due to local laser heating) and linear temperature effects were taken into account. Periodic, position-dependent absorption, defined by the optical interferometric pattern set up by the laser, was used to describe the interaction of the laser beam with the mechanical structure. The model assumed non-linearity of the oscillator. It was analytically shown that stable, self-sustained oscillations are achieved at a certain threshold of CW laser power in a Hopf-type bifurcation. This threshold was calculated to be close to the experimentally observed values. To analyze the stability of the solutions above the critical point a simplified model accounting only for parametric effects was considered. Using the method of harmonic balance it was shown that a stable limit cycle in the phase plane exists that determines the amplitude of self-oscillations.

ACKNOWLEDGEMENTS

This work was supported by the Cornell Center for Materials Research (CCMR), a Materials Research Science and Engineering Center of the National Science Foundation (DMR-0079992). Particular acknowledgment is made of the use of the Research Computing Facility of the CCMR.

REFERENCES

1. J.D. Zook, W.R. Herb, C.J. Bassett, T. Stark, J.N. Schoess, M.L. Wilson, Sensors and Actuators A 83 270-276 (2000).
2. N.A.D. Stokes, R.M.A. Fatah and S. Venkatesh, Sensors and Actuators, A 21-23, 369-372 (1990).
3. Partridge, J.K. Reynolds, B.W. Chui, E.M. Chow, A.M. Fitzgerald, L. Zhang, N.I. Maluf, T.W. Kenny, J. MEMS, 9, 58 (2000).
4. Dror Sarid, Scanning Force Microscopy With Applications to Electric, Magnetic and Atomic Forces, New York Oxford University Press (1994).
5. J.A. Sidles, J.L. Garbini, K.J. Bruland, D. Rugar, O. Zuger, S. Hoen, and C.S. Yannoni, Rev. Mod. Phys. 67, 249 (1995).
6. B. Ilic, D. Czaplewski, H. G. Craighead, P. Neuzil, C. Campagnolo, and C. Batt, Applied Physics Letters 77, 451 (2000).
7. C. T.-C. Nguyen, "Transceiver front-end architectures using vibrating micromechanical signal processors", Dig. of Papers, Topical Meeting on Silicon Monolithic Integrated Circuits in RF Systems, Sept. 12-14, 2001, pp. 23-32.
8. S. Lee, M. U. Demirci, and Clark T.-C. Nguyen, "A 10-MHz micromechanical resonator Pierce reference oscillator for communications", Digest of Technical Papers, the 11th Int. Conf. on Solid-State Sensors & Actuators

(Transducers01), Munich, Germany, June 10-14, 2001, pp. 1094-1097.
9. D. Rugar and P. Grutter, "Mechanical parametric amplification and thermomechanical noise squeezing", Phys. Rev. Lett 67, 699 (1991).
10. D.W. Carr, S. Evoy, L. Sekaric, H.G. Craighead and J.M. Parpia, "Parametric amplification in a torsional microresonator", Appl. Phys. Lett. 77, 1545, (2000).
11. A. Olkhovets, D.W. Carr, J.M. Parpia and H.G. Craighead "Non-Degenerate Nanomechanical Parametric Amplifier", IEEE Intl. Conference on Micro Electro Mechanical Systems MEMS 2001, Interlaken, Switzerland, January 21-25, 2001.
12. W.M. Dougherty, K.J. Bruland, J.L. Garbini and J.A. Sidles "Detection of AC magnetic signals by parametric mode coupling in a mechanical oscillator", Meas. Sci. Technol. 7, 1733 (1996).
13. A. Dana, F. Ho, Y. Yamamoto, "Mechanical parametric amplification in piezoresistive gallium arsenide microcantilevers", Appl. Phys. Lett. 72, 1152 (1998).
14. K. L. Turner, S. A. Miller, P.G. Hartwell, N. C. MacDonald, S. H. Strogatz, and S. G. Adams, "Five Parametric Resonances in a MicroElectroMechanical System", Nature, 396, 149-152 (1998).
15. M. Zalalutdinov, A.T. Zehnder, A. Olkohovets, S. Turner, L. Sekaric, B. Ilic, D. Czaplewski, J.M. Parpia, and H.G. Craighead, "Auto-Parametric Optical Drive for Micromechanical Oscillators", Applied Physics Letters, 79, pp. 695-697, (2001).
16. M. Zalalutdinov, A. Olkhovets, A.T. Zehnder B. Ilic, D. Czaplewski, H. G. Craighead, and J. M. Parpia, "Optically pumped parametric amplification for MEMS oscillators", Applied Physics Letters 78, pp. 3142-3144, (2001).
17. L. Sekaric, M. Zalalutdinov, S. W. Turner, A. Zehnder, J. M. Parpia and H. G. Craighead, "Nanomechanical resonant structures as tunable passive modulators of light", Applied Physics Letters, 80, pp. 3617-3619, (2002).
18. L. Sekaric, M. Zalalutdinov, R.B. Bhiladvala, A.T. Zehnder, J.M. Parpia, and H.G. Craighead, "Operation of nanmechanical resonant structures in air", Applied Physics Letters, 81, pp. 2641-2643, (2002).
19. D.W. Carr, L. Sekaric and H.G. Craighead, "Measurement of nanomechanical resonant structures in single-crystal silicon", J. Vac. Sci. Technol. B 16, 3281 (1998).
20. D.E. Gray (ed.), American Institute of Physics Handbook, 3rd ed., McGraw-Hill (1972).
21. N. Ono, K. Kitamure, K. Nakajima, and Y. Shimanuki, "Measurement of Young's Modulus of Silicon Singel Crystal at High Temperature and Its Dependency on Boron Concentration Using the Flexural Vibration Method", Japan Journal of Applied Physics, 39 (2000), pp 368-371.
22. K. Hane, "Analytical modeling of micromachined resonator sensor activated by cw laser irradiation", Transducers '97, 1997 International Conference on Solid-State Sensors and Actuators, IEEE, (1997), pp. 105-108.
23. K. Hane and K. Suziki, "Self-excited viration of a self-supporting thin film causes by laser irradiation", Sensors and Actuators A 51 (1996) pp. 179-182.